

*Active and Passive Elec. Comp.*, 1994, Vol. 16, pp. 113–117  
Reprints available directly from the publisher  
Photocopying permitted by license only  
© 1994 Gordon and Breach Science Publishers S.A.  
Printed in Malaysia

## MECHANISMS OF THE REVERSIBLE ELECTROCHEMICAL INSERTION OF LITHIUM OCCURRING WITH NCIM<sub>s</sub> (NANO-CRYSTALLITE- INSERTION-MATERIALS)

S.D. HAN, N. TREUIL, G. CAMPET,\* J. PORTIER, C. DELMAS

*Laboratoire de Chimie du Solide du CNRS, 351 cours de la Libération—33405 Talence—France*

J.C. LASSÈGUES

*Laboratoire de Spectroscopie Moléculaire et Cristalline du CNRS, 351 cours de la Libération—33405 Talence—France*

A. PIERRE

*Department of Mining—Metallurgical and Petroleum Engineering, University of Alberta—Edmonton—Alberta, T6G-2G6—Canada*

(Received September 7, 1993; in final form November 8, 1993)

A new family of insertion-compound electrodes, so called NCIM<sub>s</sub> (Nano-Crystallite-Insertion-Materials), has been proposed: the major requirement is that the electrode materials have to be polycrystalline with a crystallite and particle size as small as possible (the accepted definition being that many crystallites make a particle). Indeed, by minimizing the size of the crystallites, the formation of defects bonds is favored, particularly at the crystallite surface, acting as reversible (de)grafting sites of Li<sup>+</sup>. Also, the cation-anion bonding is weakened not only in the grain boundary region but also within the crystallite close to its surface: then the electrochemical insertion of Li<sup>+</sup> takes place through easy bonding rearrangements.

### I. INTRODUCTION

In the last 20 years, much attention has been focused on A<sub>x</sub>MO<sub>2</sub>—type intercalation compounds (A = Li, Na and M = Co, Ni, Mn. . .), which are used as positive electrodes in reversible alkali electrochemical cells (see for example refs. 1). However, a very long-term cyclability (i.e., over 10<sup>3</sup> cycles) might be hardly achievable, particularly for corresponding electrodes having a large grain size, probably because the Li<sup>+</sup> (de)intercalation process slightly perturbs the host lattice.

Some of us have patented, a few years ago, a new strategy and related experiments that have enabled us to put forward a rather new family of insertion-compound electrodes able to sustain long-term Li<sup>+</sup> electrochemical cyclability<sup>2</sup>. The major requirement is that the electrode materials are polycrystalline with a crystallite and particule sizes as small as possible. Therefore, we later called the polycrystalline electrode materials NCIM<sub>s</sub> (for nano-crystallite-insertion material)<sup>3,4</sup>.

---

\* Author for correspondence.

TABLE I  
Some nanocrystallite insertion materials (NCIMs)

Sample	Class	Average grain size (Å)	Insertion rate x (measured in LiClO <sub>4</sub> (p.c.), 1.5V ≤ V(Li) ≤ 3.5V)
Li <sub>x</sub> SrTiO <sub>3</sub>	D	80	0 ≤ x ≤ 0.3
Li <sub>x</sub> CrO <sub>2</sub>	I	30	0 ≤ x ≤ 1
Li <sub>x</sub> Mn <sub>2</sub> O <sub>3</sub>	I	50	0 ≤ x ≤ 2
Li <sub>x</sub> Fe <sub>2</sub> O <sub>3</sub>	D	150	0 ≤ x ≤ 0.5
Li <sub>x</sub> NiO <sub>2</sub>	I	60	1 ≤ x ≤ 2
Li <sub>x</sub> CuO <sub>2</sub>	I	50	1 ≤ x ≤ 2
Li <sub>x</sub> WO <sub>3</sub>	D	40	0 ≤ x ≤ 2

Table I gives important examples related to mixed-valency metal oxides<sup>2,5</sup>. For clarity, the examples listed in Table I have been divided into two classes, I and D, according to whether the resistivity tends to increase (class I) or to decrease (class D) upon the electrochemical Li<sup>+</sup> insertion process.

Rather similar considerations were reported by Barloux *et al.* and concern the spinel LiMn<sub>2</sub>O<sub>4</sub><sup>6</sup>. Also apparently related to that, Kumagai *et al.*<sup>7</sup> have reported that the positive electrode MnO<sub>2</sub>·yV<sub>2</sub>O<sub>5</sub> was formed by incorporation of V<sub>2</sub>O<sub>5</sub> into MnO<sub>2</sub> matrices and the crystallinity of the oxide decreased with increase in V<sub>2</sub>O<sub>5</sub> content incorporated. They have shown that the amount of Li<sup>+</sup> ions that can be reversibly electrochemically (de)inserted increased with increasing y value, i.e., with decrease in the crystallinity; it reached about 1 Li<sup>+</sup> per mole of the oxide with y = 0.6<sup>7</sup>.

***In this paper, the framework of the model accounting for the reversible electrochemical Li<sup>+</sup> insertion occurring in the NCIM<sub>s</sub> is presented. We also show, for the first time, that the model accounts for the evolution of the open circuit voltage of the electrodes, vs the fraction, x, of the alkali.***

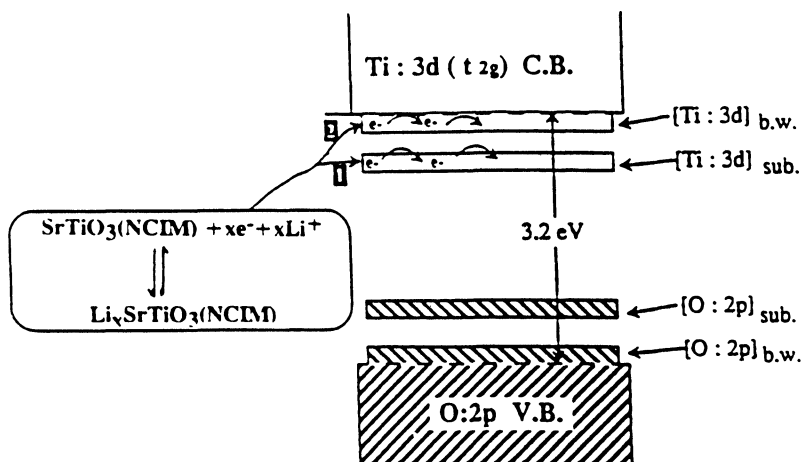
## II. MECHANISMS OF THE REVERSIBLE ELECTROCHEMICAL INSERTION OF LITHIUM OCCURRING WITH NCIM<sub>s</sub>

First of all, by minimizing the size of the crystallites we tend to:

- (i) favor the formation of defect bonds, particularly at the crystallite surface (of its vicinity), such as anion adjacent to cation vacancies: ***these defects act as reversible (de)grafting sites for Li<sup>+</sup>.***
- (ii) weaken the cation-anion bonding not only on the grain boundary region but also within the grain close to its surface: ***then the electrochemical insertion of Li<sup>+</sup> occurs through easy bonding rearrangements<sup>3</sup>.***

That is depicted below for SrTiO<sub>3</sub>-NCIM, ***taken as a non-limiting but illustrative example.*** First of all, Fig. 1 illustrates the electron conduction via [Ti:3d]<sub>sub</sub> or [Ti:3d]<sub>bw</sub> energy states.

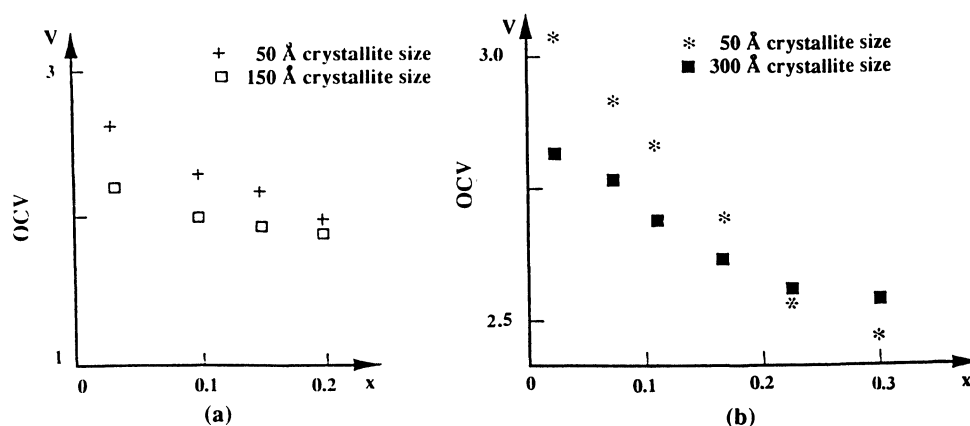
- [Ti:3d]<sub>sub</sub> represents deep subband-gap energy states arising from cation defects adjacent to an anion vacancy. They are lowered below the π\* conduction

FIGURE 1 Simplified band energy scheme of SrTiO<sub>3</sub>-NCIM.

band of Ti<sup>4+</sup>:3d<sup>0</sup>(t<sub>2g</sub>) parentage. Conversely, anion defects adjacent to cation vacancies occur. They introduce acceptor states [O:2p]<sub>sub</sub> arising from the O<sup>2-</sup>:2p<sup>6</sup> valence band. According to the model, the latter defects act as reversible (de)grafting sites for Li<sup>+</sup>, (see (i)).

- the [Ti:3d]<sub>bw</sub> and [O:2p]<sub>bw</sub> energy states originate from Ti-O bond weakening. This bond weakening induces Li<sup>+</sup> (de)insertion as mentioned above (see (ii)).

We will see, now, that the model accounts for the differences observed between the open-circuit voltage (OCV) vs x (the fraction of the alkali) curves related to polycrystalline electrodes having different sizes of crystallites. For sake of simplicity, such a behavior is illustrated only for two n-type electrodes Li<sub>x</sub>SnO<sub>2</sub> and Li<sub>x</sub>WO<sub>3</sub> (Fig. 2a, b).

FIGURE 2 Equilibrium OCVs vs x for some Li/LiCF<sub>3</sub>SO<sub>3</sub>/NCIMs (a:Li<sub>x</sub>SnO<sub>2</sub>; b:Li<sub>x</sub>WO<sub>3</sub>).

The concentration of the “sub” and b.w.” states increases as the crystallite size is reduced. This obviously causes, **only for the lower  $x$  values**, a “pushing” of the Fermi-energy ( $E_F$ ) and thereby of OCV towards “cathodic” values. Indeed, for the lower  $x$  values, the OCV are higher for the electrodes having the smallest crystallite size (Fig. 2a and 2b for  $x \leq 0.15$ ).

For higher  $x$  values ( $x \gg 0.15$ ) and when the inside-crystallite structure is well adapted for the reversible intercalation of lithium as it occurs for  $\text{Li}_x\text{WO}_3$ , an inversion of the OCV is observed (Fig. 2b): indeed for  $x \gg 0.15$  all the subband gap energy states  $[\text{W}^{6+}:5d^0]_{\text{sub}}$  and  $[\text{W}^{6+}5d^0]_{\text{bw}}$  (the “twin states” of  $[\text{Ti}^{4+}:3d^0]_{\text{sub}}$  and b.w. reported in Fig. 1) are filled with electrons. Therefore, the lithium intercalation within the nanocrystallites can now take place; it is accompanied with a “delocalization” of the injected electrons in the conduction band. On the other hand, it is well established that the band-energy width increases as the crystallite size decreases [8]; therefore the  $\text{WO}_3$  electrodes having the smallest crystallite size have their conduction-band edge shifted towards “anodic” values: this causes a “decrease” of  $E_F$ , and thereby of OCV, towards “anodic” values (as it is illustrated on Fig. 2b for  $x \gg 0.15$ ).

### III. THE NCIM HAVE BEEN INVESTIGATED IN DIFFERENT FORMS: EITHER POWDERED ELECTRODES (A) OR COMPOSITE ELECTRODES (B) OR THIN FILM ELECTRODES (C).

#### 1. Powdered Electrodes or Composite Electrodes

They can be efficiently used as positive electrodes for rechargeable lithium batteries of high energy density. Figure 3 shows the charge-discharge curves for powdered and composite electrodes.

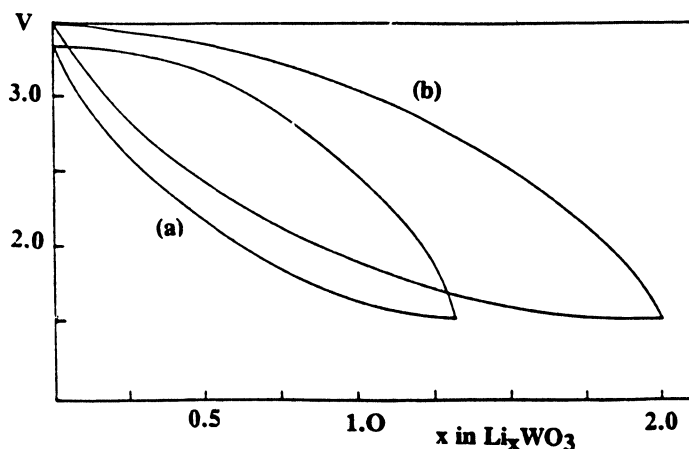


FIGURE 3 Charge-discharge curves of: (a)  $\text{Li}/\text{LiClO}_4\text{-p.c.}/\text{WO}_3\text{-NCIM}$  ( $50\text{\AA}$  size), (b)  $\text{Li}/\text{LiClO}_4\text{-p.c.}/\text{'soft'}$  composite electrode consisting of  $\text{WO}_3\text{-NCIM}$  ( $50\text{\AA}$  size) dispersed in conductive polymer.

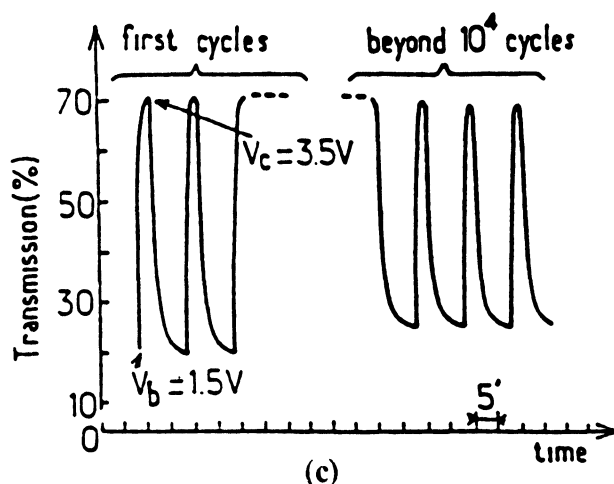


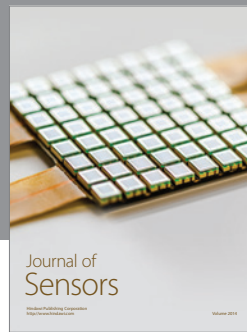
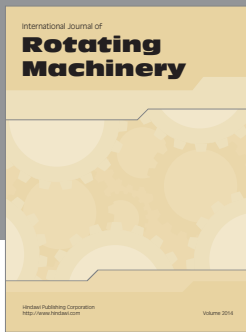
FIGURE 4 Transmission ( $\lambda = 550$  nm) vs time for repeated coloring and bleaching cycles with the NCIM ( $50 \text{ \AA}$ ) counter electrodes  $\text{Li}_{2-x}\text{NiO}_2$  (c). The  $\text{Li}^+$  insertion rate,  $x$ , varies within 0 and 1. The coloring and bleaching potentials  $V_c$  and  $V_b$  are measured vs Li in  $\text{LiClO}_4$ , p.c. electrolyte.

## 2. Thin Film Electrodes

They can be efficiently used either as positive electrodes for thin-film rechargeable batteries of high energy density or as counter electrodes for electrochromic windows. Transmission vs time for repeated coloring and bleaching cycles is shown in Figure 4.

## REFERENCES

1. J. Rouxel, in F. Levy (ed.), *Physics and Chemistry of Layered Materials*, vol. VI, Reidel, Dordrecht, 1979.  
K. Mizushima, P.C. Jones, P.J. Wiseman and J.B. Goodenough, *Solid State Ion.*, 3-4 (1981) 171.  
C. Delmas, J. Braconnier, A. Maazaz and P. Hagenmuller, *Rev. Chem. Miner.*, 19 (1982) 343.  
J. Molenda, *Solid State Ion.*, 21 (1986) 263.  
S. Miyazaki, S. Kikkawa and M. Koizumi, *Synth. Met.*, 6 (1983) 211.
2. J.P. Couput, G. Campet, J.M. Chabagno, M. Bourrel, D. Muller, R. Garrié, C. Delmas, B. Morel, J. Portier and J. Salardenne, *Int. Appl. Publ. under PCT. Int. Pat. Class GO2F 1701, FO1 G9/00, C 23C 14/34, WO 91/01510*, 1989.
3. N. Treuil, G. Campet, unpublished results: DEA report of N. Treuil. Bordeaux (1993).
4. G. Campet, S.D. Han, N. Treuil, MCR Shastry, J. Portier, C. Delmas, J.C. Lassègues, *Mat. Sciences and Eng. B* (submitted for publication).
5. B. Morel, Doctoral thesis, University of Bordeaux I (1991).
6. P. Barloux, J.M. Tarascon and F.K. Shokoohi, *J. Solid State Chem.* 94 (1991) 185.
7. N. Kumagai, S. Tanifuji, T. Fujiwara and K. Tanno, *Electrochim. Acta*, 37(6) (1992) 1039.
8. P.E. Lippens and M. Lanoo, *Physical Review B*, 39 (1989) 15.



**Hindawi**  
Submit your manuscripts at  
<http://www.hindawi.com>

